Journal of Membrane Science & Research

journal homepage: www.msrjournal.com

Research Paper

Evaluation of a Quaternized Polyethersulfone Membrane Enhanced with Amine Functionalized Carbon Nanotubes for Forward Osmosis Application

Vhahangwele Mudzunga [1,2], Richard Motlhaletsi Moutloali [1,2], Phumlani Fortune Msomi [1,2,3,*]

[1] *Department of Chemical Sciences, University of Johannesburg, Johannesburg, South Africa*
[2] *DSI/Mintek Nanotechnology Innovation Center- UJ water Research Node, University of Johannesburg, Johannesburg, South Africa*
[3] *Centre for Nanomaterials Science Research, University of Johannesburg, Johannesburg, South Africa*

Article info

Received 2020-10-05
Revised 2020-11-13
Accepted 2020-11-25
Available online 2020-11-25

Keywords

Polyethersulfone
Carbon nanotubes
Forward osmosis
Reverse solute flux
Conductive membrane

Highlights

- Quternized CNTs increases membrane basic properties
- New QPES/QCNTs composite membrane fabricated
- QPES/QCNTs with enhanced antifouling properties
- QCNTs improved reverse solute flux compared to pristine CNTs

Graphical abstract

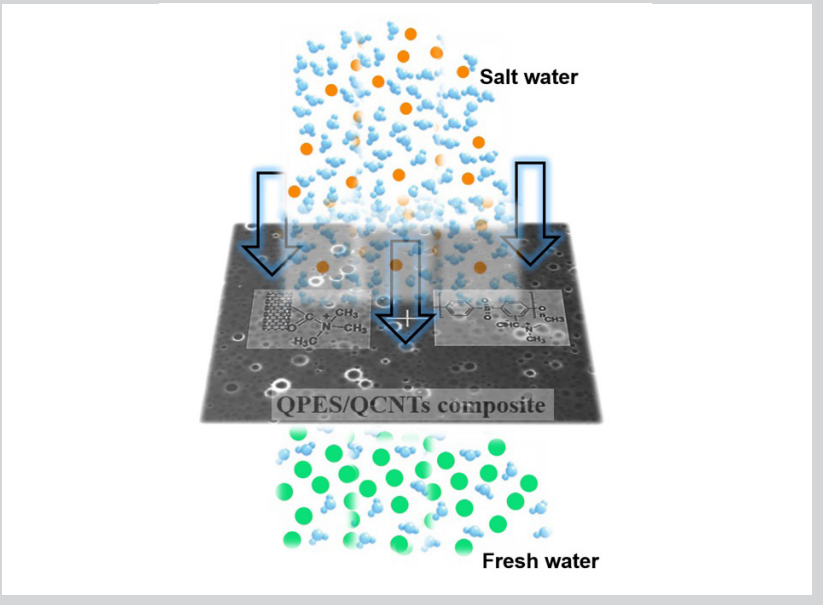

Abstract

Multiwall carbon nanotubes (CNTs) were quaternized (QCNTs) with trimethylamine to form an anionic conductive CNTS then blended with quaternized polyethersulfone membrane (QPES) by phase invasion method to obtain a composite membrane with higher permeation, improved rejection and enhanced antifouling properties for forward osmosis application. The membranes and QCNTs were characterized using SEM, TGA, NMR, Raman and FTIR. The fabricated composite membranes showed that addition of QCNTs can improve membrane basic properties when compared to commercial polyethersulfone membranes. This observed improvement could be attributed to the incorporated oxygen and amine functionalities in the CNTs. The 0.1 wt % QCNTs showed a contact angle of 64º, reverse solute flux of 7.4 and 6.2 $Lm^{-2}h^{-1}$ for NaCl and $MgSO_4$ respectively compared to an original pure water flux of 8.058 $Lm^{-2}h^{-1}$. Humic acid was used as a foulant, when the composited was fouled using humic acid, the 0.1wt.% QCNTs showed a reverse solute flux of 5.7 and 5.0 $Lm^{-2}h^{-1}$ respectively at room temperature.

1. Introduction

Water scarcity continues to increase around the globe due to various reasons related to population growth, increasing living standards and global warming [1]. This makes the quality of freshwater in the world to remain a critical issue. In South Africa, the quality of drinking water is deteriorating daily, especially in rural areas where water is polluted and contaminated by the nature of living conditions [2,3]. Reverse Osmosis currently holds the majority of world water purification systems since it is a proven technology for water purification. Due to high energy requirements in the use and production of RO systems, this has paved way for other emerging membrane technology such as forward osmosis (FO) which has a very low energy demand [4]. FO is a less intensive process and uses osmotic pressure [5]. This process utilizes the osmotic pressure that occurs between the feed solution and draws solution placed on the opposite sides of the membrane [5,6]. Internal concentration polarization and fouling is, however, still a serious factor limiting the use of FO membrane technology [7]. To address the problem of fouling and internal concentration polarization, cellulose acetate membranes have been used due to their hydrophilic nature. The membrane showed reduced internal concentration polarization (ICP) and increased

* Corresponding author: pmsomi@uj.ac.za (P.F. Msomi)

DOI: 10.22079/JMSR.2020.137656.1413

water flux for osmotically driven membranes [8]. Polyethersulfone membrane has also been used widely for fabrication of forward osmosis membrane due to tremendous properties such as good thermal, mechanical and oxidative properties with high glass temperature [9]. The major drawback of PES is that they are hydrophobic which limits their properties during the water application filtration process which further reduces its performance [10]. On the other hand the use of CNTs technology has played a big role in improving polymer properties due to their exceptional high ratio in combination with low density, high strength and stiffness which makes CNTs to be more preferred additives in polymers [11].

Goh et al. [12] investigated the transport of water in a polymer composite blended with CNTs and obtained excellent flux for desalination membranes. Literature has also reported that CNTs are the better nanofiller for composite membranes due to the transport rate of water caused by the smoothness of the nanotube and its compatibility with a variety of polymers [13]. Qiu et al. [14] observed that the incorporation of multiwalled CNTs enhances membrane structure and filtration performance. Ge et al. [15] also fabricated PES/CNTs composite membrane, the membrane showed stronger CNTs interactions with CO_2 to enhance water permeability. Choi et al. [11] showed that modification of polyethersulfone membrane with functionalized CNTs improves membrane flux and surface hydrophilicity. The results showed that the modified nanocomposite membrane exhibit a high hydrophilic performance upon incorporation of CNTs than pure PES. These studies focused on cellulose acetate membrane. FO membrane are considered a bench mark in the field of water treatment due to good mechanical strength and lower fouling propensity unlike thin film composite FO membrane possess a vulnerable active polyamide active layer [16]. In this work, we look at changing PES hydrophobic nature and make it hydrophilic by tendering cation moieties on its surface. The CNTs were also functionalized with the same cation moieties then blended with the anionic PES. This resulted in a highly hydrophilic membrane that lead to enhance properties such as flux, reverse solute flux and antifouling properties, thereby providing an efficient membrane for the FO system.

2. Experimental

2.1. Materials

The reagents used for this research study included 1,1,2,2-tetrachloroethane, sulphuric acid, thionyl chloride, nitric acid, zinc chloride, N-methyl-2-pyrrolidone, chloromethyl ethyl ether, trimethylamine (25 wt.% in water), potassium hydroxide, carbon nanotubes purchased from Sigma-Aldrich, Johannesburg, South Africa. Polyethersulfone (PES, was acquired from Solvay Advanced Polymers (South Africa). All chemicals were used without further purification or modification.

2.2. Functionalization of multi-walled carbon nanotubes (CNTs)

The multiwalled carbon nanotubes were functionalized by adding CNTs (2.0 g) into a solution of HNO_3 / H_2S0_4 (20 mL) mixture and stirred under reflux for 24 h at 90 °C. The functionalized CNTs were filtered and washed with distilled water until the pH of the water released after washing was neutral. The functionalized CNTs were dried in an oven at 100 °C for 10 h. The dried CNTs were then soaked in a solution of thionyl chloride 30 wt % to chlorinate some of the carboxylic acid groups to promote nucleophilic substitution with trimethylamine (TMA). The chlorinated CNTs were then soaked in trimethylamine (30 wt %TMA, for 24 h at room temperature to ensure the quarterization of the CNTs (QCNTs) [17]. The TMA-CNTs were then dried and stored in the locker for later use. Figure 1 below shows the preparation of TMA functionalized CNTs (QCNTs) [18].

2.3. Chloromethylation of polyethersulfone (PES-Cl)

The polyethersulfone (PES) was chloromethylated by dissolving 2.0 g PES in 1,1,2,2-tetrachloroethane (16 mL) while stirred under reflux in nitrogen gas condition for 12 h at 70 °C. Then thionyl chloride (1.5 mL) was added slowly, zinc chloride solution (1.1 mL) was also added while continuously stirring the solution. Four drops of chloromethyl methyl ether (CMEE) was then added dropwise into the reaction flask. The reaction mixture was allowed to stir for another 6 h at 70 °C. The solution was then cooled at room temperature and subsequently precipitated with methanol. A yellow fibrous solid polymer was obtained indicating successful chloromethylation of PES [19]. Figure 2 schematic diagram shows how chloromethylation was achieved.

2.4. Fabrication of quaternized PES blended with quaternized CNTs composite membrane

The quaternized PES blended with quaternized CNTs (QPES/QCNTs) membranes were prepared by the solvent induced phase inversion method [20]. Quaternized carbon nanotubes (QCNTs) were obtained in three different weight variations (0.1 wt.%, 0.3 wt.% and 0.5 wt.%) dispersed in different conical flask containing the required volume of N-Methyl-2-pyrrolidone (NMP) solution and sonicated for 1 h. PES-Cl was added to the stirring mixture of QCNTs having various fractions, each stirred for 24 h to obtain a homogenous nanocomposite membrane. The obtained composite solution was then cooled and cast on a glass plate then phase inversion method used to obtain a free stating membrane.

2.5. Characterizations and evaluation of all membranes

2.5.1. Membrane characterization

The morphology of all membranes was characterized using the SEM JEOL 5600. Samples were prepared by mounting on aluminium studs with carbon tape. Prior to analysis, samples were coated with carbon. Samples for cross-section all studied were cryogenically fractured in liquid nitrogen, securely mounted on aluminium studs and then coated with gold, in order to induce their capacity to conduct. The LEO 912 TEM was used to estimate the particle size of the QCNTs and observe the morphology of the QCNTs. The QCNTs were suspended in methanol for 11.4 minutes in an ultrasonic bath to obtain a homogeneous dispersion of each sample, followed by dropping some suspension onto a copper grid placed into the TEM chamber. Raman spectra were collected from a Perkin Elmer Raman microscope 200 technique at an excitation source of 785 nm and fine powdered dried samples of quaternized focused on a laser beam of 5Mw over an average of 50 to 3500 cm^{-1} with a resolution of 2.0 cm^{-1}, a spectral average of 22 scans and an exposure time of 4 s. The NMR spectra of PES, PES-Cl and QPES were obtained with a ^{1}H-NMR spectrometer (Bruker Avance III HD NMR 500 MHz, equipped with BBO probe) using deuterated dimethyl sulfoxide as the solvent. The Perkin Elmer Spectrum (version 10.4.2) instrument with a horizontal ATR device at the scan range of 650- 4000 cm^{-1}, the resolution of 4 cm^{-1} and over a range of 16 scans. QCNTs were characterized as powder and PES composites as a solid membrane. TGA data were obtained with model STA (Simultaneous Thermal Analyser) 1500 (supplied by Rheometric Scientific Ltd, UK), at a heating rate of 10°C.min^{-1}. The samples were heated from 50 – 1000°C.

2.5.2. Membrane evaluation

The wettability and surface hydrophilicity of the PES and QPES/QCNTs membranes were evaluated by the DATA Physics optical contact angle using the sessile drop measurement method. An average contact angle (θ) of 10 drops of deionized (DI) water was placed on a flat membrane surface using a Gilmont syringe. Using the SCA20 version 4.1.12 build 1019 software, the advancing angle (θ) was measured as the water droplet was placed on the surface.

Membrane performances of the QPES/QCNTs were studied by pure water flux. The forward osmosis system is operated with two tanks, one with a draw solution and one with a feed solution separated by the membrane. The membrane was placed on the membrane chamber of the forward system with an area of 25 cm^2. The flow rate was kept constant through the operation at 2 $L.min^{-1}$. The draw solution and the feed solution were prepared from a solution of 2 M and 1 M respectively consisting of different draw solute per initial run. Magnesium sulphate (MgSO4) and Sodium chloride (NaCl) were chosen as a draw solute in this study as they exhibit high osmotic pressure due to their high-water solubility.

The performances of the QPES/QCNTs membranes were studied by measuring the pure water flux and rejections. Water flux was obtained by measuring the weight change of the feed solution over a selected period (30 min). The membranes were pre-conditioned by compacting with deionized water at an osmotic pressure until steady fluxes were obtained. Water flux (J_w) was calculated using Equation 1:

$$Jw = \frac{\Delta V}{Am \times \Delta t} \quad (1)$$

where V (L) is the volume of the permeation water. Am (m^2) is the area of the membrane, and ΔT (h) is the time taken to acquire each measurement. Reverse solute flux can be described as the measure of solute from a higher concentration called draw solution passing through the forward osmosis membrane to a lower concentration called feed solution.

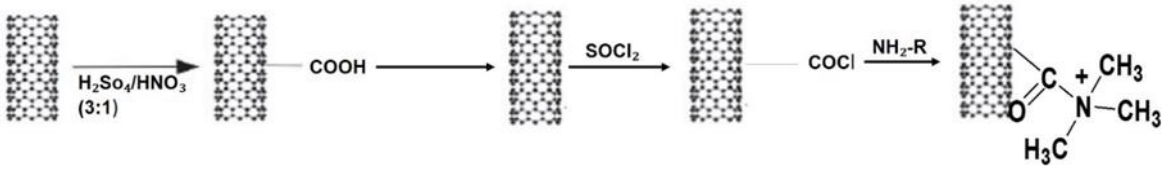

Fig. 1. Schematic diagram of the functionalization of CNTs.

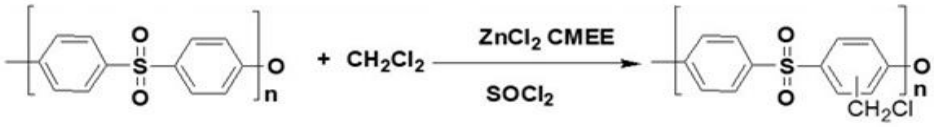

Fig. 2. Chloromethylation of polyethersulfone (PES).

The reverse solute flux was calculated by the change of NaCl and $MgSO_4$ concentration in the feed solution. The reverse solute was calculated using Equation 2 as showed below:

$$Js = \frac{\Delta(Ct \times Vt)}{Am \times \Delta t} \quad (2)$$

where C_t and V_t are the salt concentration and the volume of the feed at the end of FO tests, respectively. At least five samples were tested and the average value was obtained for each membrane.

Fouling experiment was performed with deionized water as a feed solution and draw solution of a single salt of NaCl and $MgSO_4$. The concentration of each salt per experiment was 2.0 M on the draw solution and 1.0 M on the feed solution. A new membrane was placed in the FO system and subjected to pure water flux measurement (Jw for 1). 2 L of a 2.0 M draw solution was added to the draw tank and 2 L of a 1.0 M feed solution was added to the feed tank. A 50 ppm humic acid solution was poured into the 1.0 M feed tank to evaluate antifouling properties.

3. Results and discussion

3.1. TEM Analysis of CNTs

Figure 3 (a-b) presents transmission electron microscopy (TEM) images of CNTs and QCNTs. Figure 3a shows tubular bundles of pristine (CNTs) in line with literature reports [21]. Figure 3b presents the TEM images of the quaternized CNTs. The quaternized CNTs exhibits an increase on dispensation, this observation was attributed to the increase of oxygen functional groups and amine functional groups within the surface of the tubes as a result of functionalization with acid and quarterization with amine [22,23].

Figure 3c, is the size distribution of the outer diameter for both CNTs and QCNTs. Java –based image (Image J) software was used to observe changes on the outer diameter of the tube after modification and this was confirmed by TEM micrographs (Figure 3a and Figure 3b) The quaternized carbon nanotubes (QCNTs) show a diameter decrease at ranges of 1-10 nm,10-20 nm compared to pristine CNTs which is attributed to interaction with outermost graphene layers [24]. The outer diameter ranging from 30 - 40 nm and 40 - 50 nm increased due to the non-sp^2 carbon defects present on the CNTs and such defects is caused by highly reactive active atoms such as carbon chains [25,26].

3.2. Raman analysis of CNTs

Figure 4 shows a Raman spectrum during QCNTs synthesis. The spectra generally showed two characteristics peaks called D-band and the G - band. The variable peaks (1579 cm^{-1}, 1578 cm^{-1} and1345 cm^{-1}) are assigned to the D- band. The D- band was attributed to the C=C stretching vibration of the graphitic carbon nanotubes which is a significant characteristic of sp^2 hybridization of carbon material. Moreover, the D-band was attributed to the defects induced by the presence of the incorporated oxygen and amine functional groups on the carbon nanotubes. The other variable peaks (1347 cm^{-1},1351 cm^{-1}, and 1345 cm^{-1}) are assigned to the G-band. The G- band corresponds to the structural disorder because it contains impurities and the presence of amorphous carbon in CNTs samples and also the sp^3 hybridization of carbon material.

The G-band at 1574 cm^{-1} corresponds to the tangential mode of CNTs. Raman spectrum showed a higher intensity of the G- band when compared to the D- band, in addition, G- band has two characteristics peak the G- band and the G' band. The variable G' band peaks (2680 cm^{-1}, 2687 cm^{-1} and 2665 cm^{-1}) are assigned to the stretching vibration of C=C These were due to poor structural quality of the carbon nanotubes samples [22,25,27-33]. The emergent peak at 2927 cm^{-1} is assigned to the oxygen functionalities and also the peak at 2922 cm^{-1} is assigned to the chlorine group introduced. These are attributed to structural defects [34]. Raman show successful chemical functionalization of CNTs to QCNTs.

Table 1 below shows the position of D and G band as well as the area ratio for CNTs and QCNTs. The area ratio of I_D/I_G ratio used to estimate the amount of disorder present in the wall of CNTs. A higher I_D/I_G ratio (0.86) was observed when CNTs were functionalized with acid. These are attributed to the introduction of functional groups –OH and –COOH form during CNT oxidation. Raman ratio of pristine CNTs is the lowest (0.84) these implies that acid functionalized carbon nanotubes were more disordered and there was also an increase sp^3 carbon on the nanotube. However, QCNTs showed the same I_D/I_G ratio as the one for acid functionalized carbon nanotubes indicating successful functionalization [32,34].

3.3. FTIR analysis of PES, PES-Cl and QPES

The FTIR spectra of PES, PES-Cl and QPES polymers are shown in Figure 5. Ccomparing PES and PES-Cl, there is an additional peak at 787 cm^{-1} for the PES-Cl membrane corresponding to the CH_2-Cl (C-Cl) stretching. This indicates successful chloromethylation of PES [35-37]. When the PES-Cl is quaternized, using trimethylamine, the peak at 787cm^{-1} (C-Cl) diminishes and a new peak at 1671 cm^{-1} appears indicating a presence of a C-N bond, C-N stretching vibrations. This indicates successful quarterization of PES [38-41].

3.4. Proton NMR analysis of PES, PES-Cl and QPES membrane

The ^{1}H-NMR spectra are in agreement with the FTIR. The NMR for PES, PES-Cl and QPES are shown in Figure 6, comparing PES and PES-Cl, a new peak is observed at about 4.95 ppm indicating the presence of protons in CH_2Cl, indicating successful chloromethylation of PES [36,42,43]. To verify successful quarterization, additional peaks for QPES can be observed at 3.81 and 3.3 ppm when compared with the PES-Cl. The 4.3 ppm peak of CH_2Cl also disappeared. This indicates a successful quarterization of PES [44]. The proton NMR in agreement with the FTIR, both indicated success in chemical grafting of trimethylamine on the backbone of the PES.

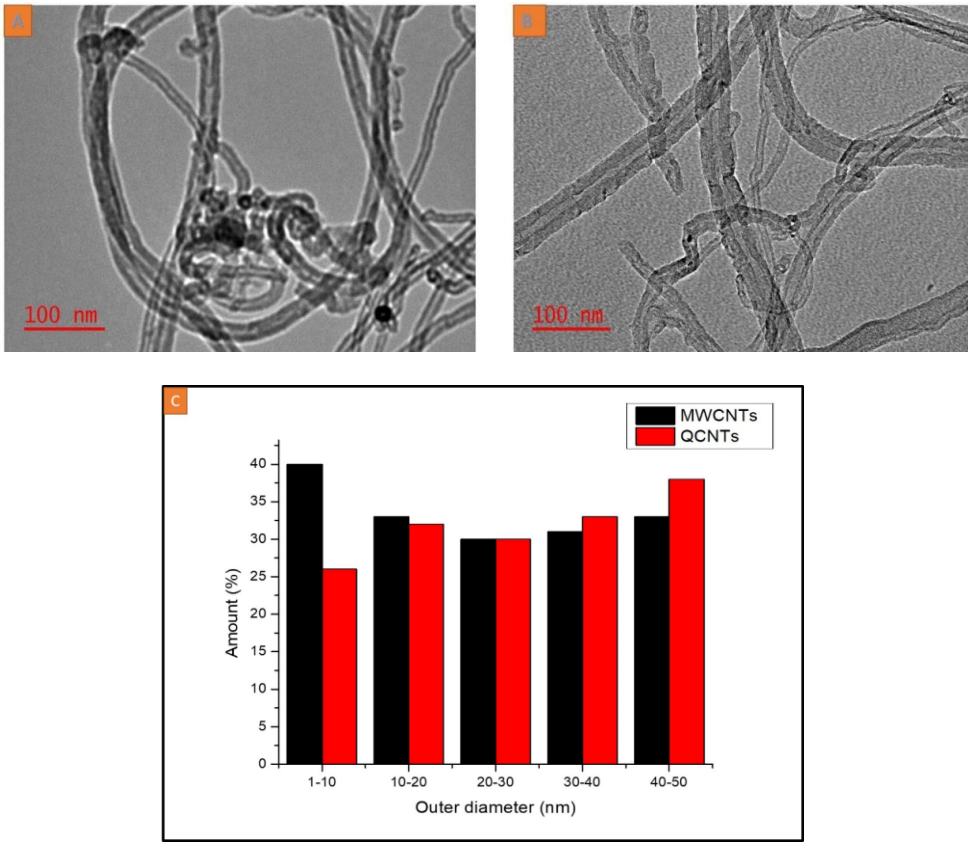

Fig. 3. TEM images of (a) pristine CNTs, (b) quaternized CNTs and (c) size distribution of the outer diameter of CNTs before and after quarterization.

Table 1
The I_g/I_d ratio of pristine CNTs and functionalized CNTs.

Sample	Peak position (cm^{-1}) D-band	Peak position (cm^{-1}) D-band	Id/Ig
P-CNT	1338.89	1579.77	0.84
F-CNT	1351.03	1571.81	0.86
CNT-Cl	1341.52	1570.21	0.85
QCNTs	1345.76	1576.35	0.85

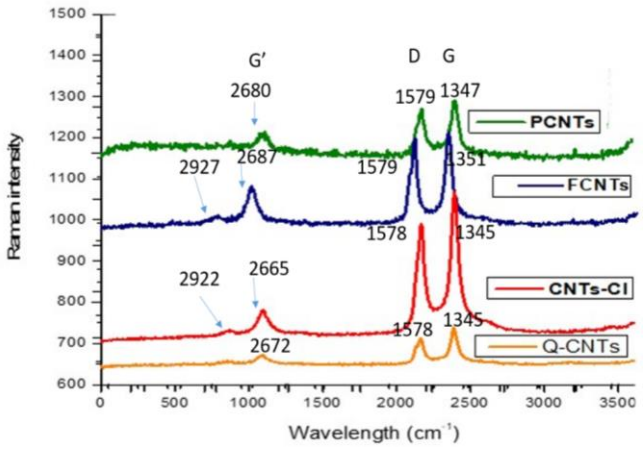

Fig. 4. Raman spectroscopy of pristin CNT (PCNTs), fuctionilized CNTs (FCNTs), chlorinated CNTs (CNTs-Cl) and quaternized CNTs (QCNTs).

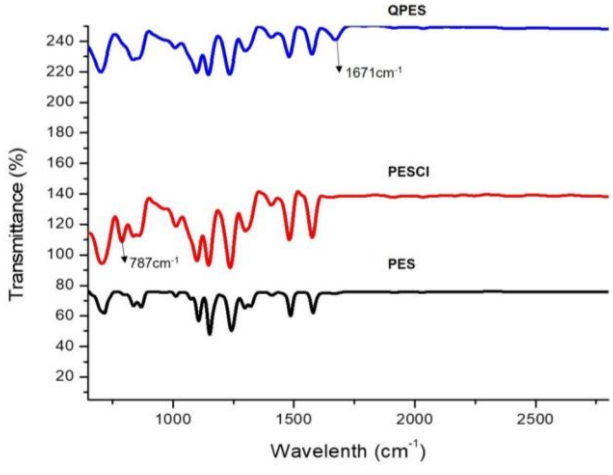

Fig. 5. FTIR spectra of PES, PES-Cl and QPES.

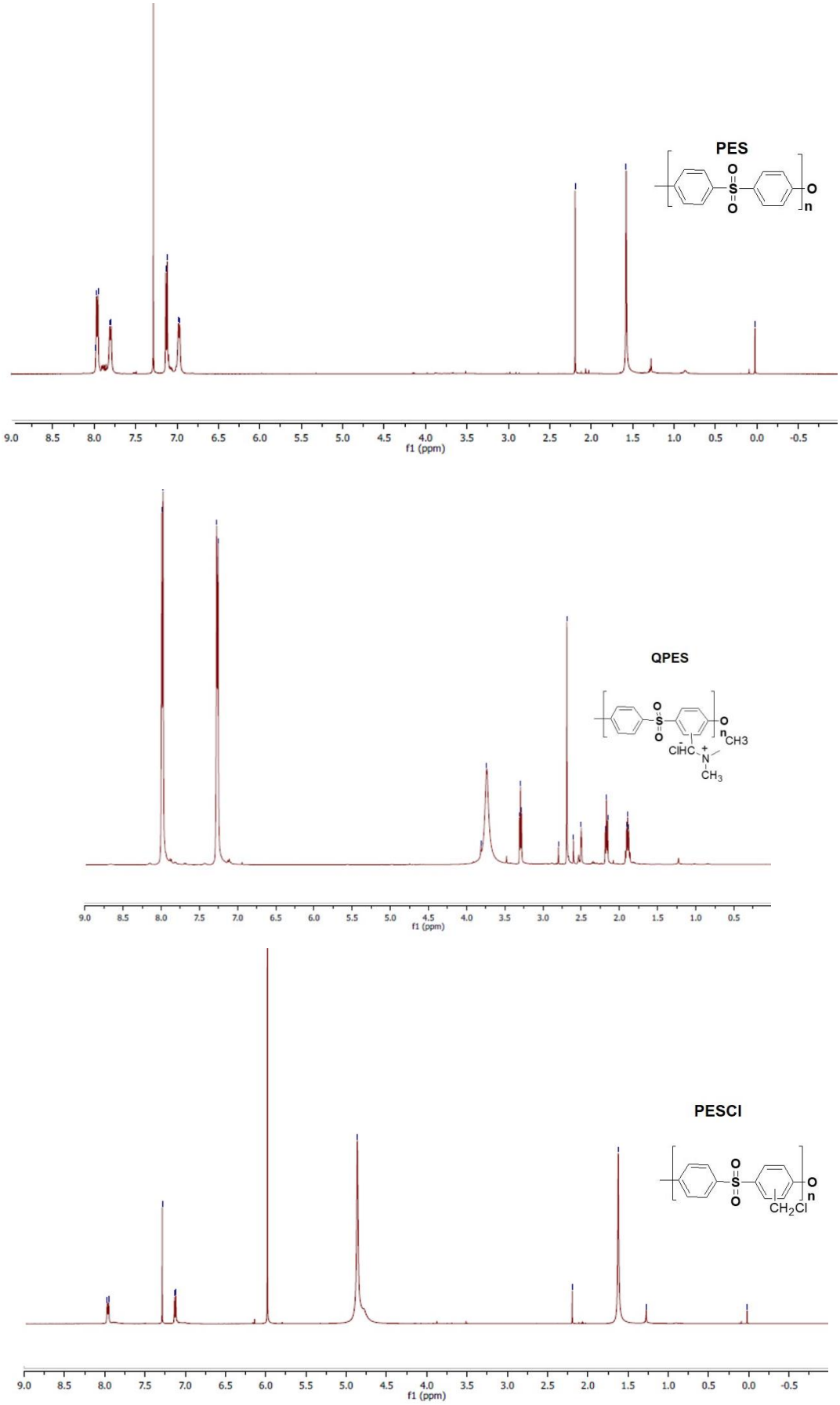

Fig. 6. HNMR spectra of PES, PES-Cl and QPES.

3.5. SEM analysis of all membranes

The surface morphology and cross-section of all membranes are depicted in Figure 7 using SEM. The surface of pristine PES showed a smooth and even surface as shown in Figure 7a, Figure 7f shows an asymmetric structure which is spongy-like which is a typical feature for PES membranes. There was no distinct difference observed in the cross-section structure between the pristine PES and the QPES/QCNTs blend membranes, however, the QPES/QCNTs membranes look more porous than the pristine PES.

In Figure 7 b-g 0.1 %QCNTs shows a smooth surface with no cracks and no indication of QCNTs agglomeration. The surface also shows the asymmetric structure of the pores. However, the membranes with 0.3% and 0.5% QCNTs in Figure 7 c-d shows agglomeration of the QCNTs on the surface. These were attributed to the untreated nanoparticle between the interfacial defects and also as the concentration of CNTs was increased, macro voids developed. Agglomeration limits the function of the CNTs and renders them less effective [45-47].

3.6. Thermal stability of all membranes

Figure 8 shows the TGA plots of all the membranes. From the graph the first 5% weight lost between 100 to 150°C can be attributed to the dehydration of water molecules held in the PES and the interlayer gallery of the carbon nanotubes due to the hydrophilic groups present [48,49]. And also, between 100 and 200°C, the loss of labile oxygen functional groups (-OH and -COOH) are observed for different weight of QCNTs modified PES as different mass losses in line with the filler loading. Between 500 and 680°C the fast loss in the weight composition of the unmodified and quaternized PES membrane is due to the degradation of the polymer residues and QCNTs [49-52]. The TGA profile indicates that the composite membranes are durable and stable up to 180°C thereby can be used for water desalination applications regardless of the water temperature.

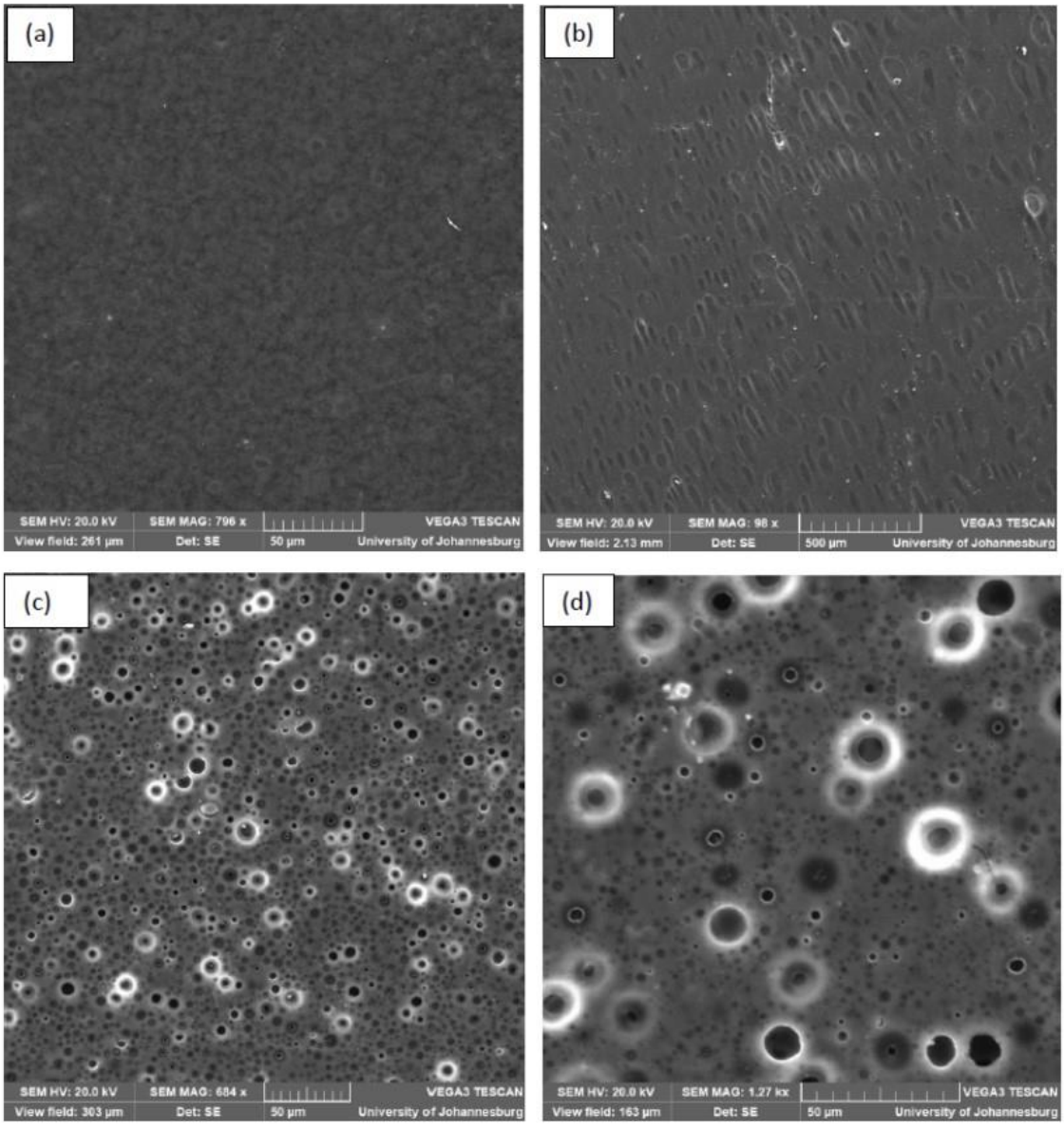

Fig. 7. SEM images of membrane surface and cross-section for; Pristine (a and f), 0.1% QPES/QCNTS (b and g), 0.3% QPES/QCNTS (c and h) and 0.5%QPES/QCNTS (d and i).

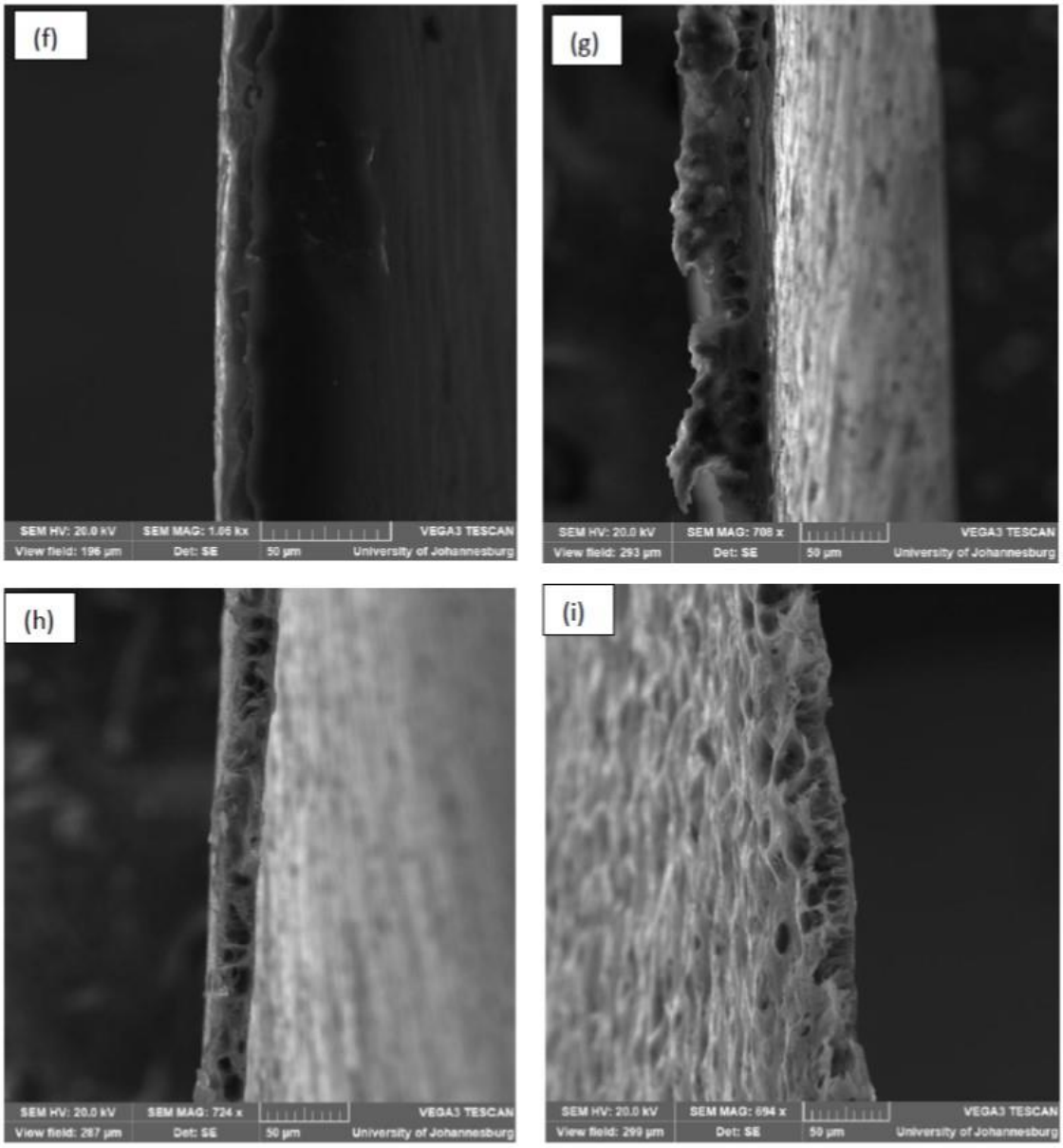

Fig. 7. Continued.

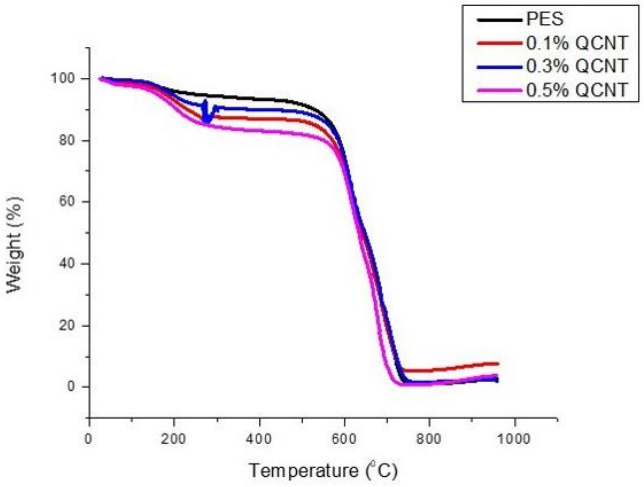

Fig. 8. TGA plots for all membranes.

3.7. Membrane evaluation

3.7.1. Contact angle, reverse solute flux and reverse solute flux after fouling

To investigate the effect of QCNTs on the membrane performance, the contact angle and forward osmosis system were used. Flux, solute rejection and fouling studies were evaluated using a forward system at atmospheric pressure with a speed of 2 $L.min^{-1}$ at a maintained temperature of 25 °C.

3.7.2. Contact angle

Figure 9 shows the contact angle of the all membrane. The contact angle of pristine PES is higher indicating the relative hydrophobicity of the polyethersulfone membrane surface. However, the addition of QCNTs decreased the contact angle indicating that QCNTs change the PES membrane to hydrophilic. The membrane with 0.1 wt.% QCNTs showed the contact angle of about 64°, was the lowest, making it the most hydrophilic membrane in this study.

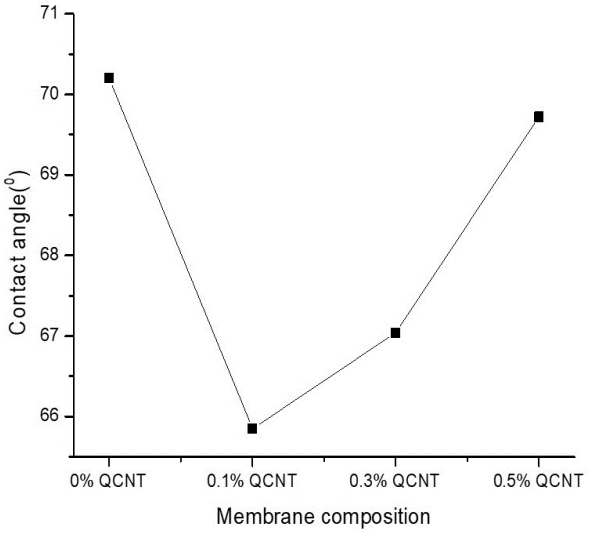

Fig. 9. Contact angle PES and of composite membranes.

The significant decrease in contact angle value can be attributed to the presence of the incorporated hydrophilic and functional groups such as C=O, C-O, -OH, -CN and -NH present on the surface of the QCNTs. In addition, these could be linked with the SEM surface morphology; the membrane with 0.1 wt.% QCNTs didn't have any agglomeration thereby indicating a perfect membrane system for this work. The membranes with 0.3 wt.% QCNTs and 0.5 wt.% QCNTs indicated agglomeration as per SEM surface morphology, which is why even though they have a high amount of QCNTs they still reported higher contact angles of about 67° and 69.6° respectively. Based on the contact angles, the membrane with 0.1 wt.% QCNTs is expected to be the most performing membrane in reverse solute flux studies [48, 53, 54].

3.7.3 Pure water flux of membranes

Membrane performances of the QPES/QCNTs were studied by pure water flux. The membrane was placed on the membrane chamber of the forward system with an area of 25 cm^2. The flow rate was kept constant through the operation at 2 $L.min^{-1}$ at room temperature. The draw solution and the feed solution were prepared from a solution of 2 M and 1 M at osmotic pressure of 24 bar and 48.9 bar respectively consisting of different draw solute per initial run [53, 55]. The highest pure water flux of 8.06 $L.m^{-2}h^{-1}$ was obtained at a loading of 0.1% QCNTs compared to pristine membrane with water flux of 7.24 $L.m^{-2}h^{-1}$ (Figure 10), which was expected based on the contact angle results in Figure 9. The membranes with 0.3% and 0.5% QCNTs showed the same trend as it did on the contact angle. The membrane with 0.3% QCNTs had a better pure water flux of 6.72 $Lm^{-2}h^{-1}$ than the membrane with 0.5% QCNTs that had a flux of 5.2 $Lm^{-2}h^{-1}$. This indicates that any further loading of CNTs can lead to a decrease in flux. The flux for 0.1% QCNTs membrane was higher than that of the pristine PES despite the lowest loadings [56].

According to literature, there are two factors, which influence the permeation properties of membranes blended with CNTs, (1) hydrophilicity and (2) pore effect. This is because the hydrophilicity of the membrane increases the number of pores on the membrane surface, therefore increasing the flux. This is why the membrane with 0.1% QCNTs has the highest flux [57].

3.7.4. Reverse solute fluxes studies of PES and composite membrane

The reverse solute fluxes for unmodified and modified PES membranes are presented below. The solute that tends to build upon the feed solution during evaluating the performance of the membrane result in reverse solute flux. According to Ambrosi et al., reverse solute flux can be described as the movement of solute from a higher concentration of draw solution to a lower concentration of feed solution [58]. Mechanism of reverse solute affect membrane properties. These result in a trade-off between reverse solute flux and internal concentration polarization because they both depend on the size of the draw solute. However, a draw solute that has high solubility and low molecular weight can drive the process at higher osmotic pressure, selecting such a draw solute will results in a membrane with higher permeate fluxes and lower internal concentration polarization [59-61].

The reverse solute flux properties of the PES and QPES/QCNTs composite membrane were evaluated using a 1.0 M concentration in the feed and 2.0 M concentration in the draw solution. The reverse solute fluxes were monitored using NaCl and $MgSO_4$ as rejection species. The membrane with 0.1 wt% QCNTs had a reverse solute water flux of 7.43 and 6.21 $Lm^{-2}h^{-1}$ for NaCl and $MgSO_4$ respectively compared to an original pure water flux of 8.06 $Lm^{-2}h^{-1}$. Pure water flux values were higher which could be due to less internal concentration polarization. This indicates better rejection properties of the membrane.

As per Figure 11, the reverse solute flux for 0.3 wt.% QCNTs membrane using NaCl and $MgSO_4$ as draw solutes was 3.92 and 4.54 $L.m^{-2}h^{-1}$ respectively. The membrane with 0.5 wt.% QCNTs also using NaCl and $MgSO_4$ as a draw solute reverse solute flux continuously decreases to 3.51 and 3.52 $L.m^{-2}h^{-1}$. These could be due to internal concentration polarization which leads to lower flux as compared to a pure flux of 8.06 $L.m^{-2}h^{-1}$ [62]. Internal concentration is the solute that builds upon the active layer on the membrane, these was observed when a 99% flux declined was obtained in an experiment which resulted by the increase on internal concentration polarisation [63]. Akther et al. [64] studied the effect of internal concentration polarization on polyethersulfone membrane, the study resulted in a more than 80% decline of reverse solute flux due to high internal concentration polarization. Based on Figure 11, which outlines reverse solute studies, the membrane with 0.1 wt.% QCNTs showed better reverse solute flux compared to the rest of the membranes.

These results indicate that a lower loading of QCNTs (0.1 wt %) renders the draw solute to create a higher osmotic pressure which will ease the solute build up on the feed draw solution. The reverse solute flux is directly proportional to salts rejection, thereby based on these results, the membrane with 0.1 wt.% QCNTs have a better salt reverse solute rejection capacity than the rest of the membranes. It has also been observed through reverse solute flux studies, at a higher loading of more than 0.3wt % QCNTs using $MgSO_4$ as a draw solution had the higher reverse solute flux. These is due to the properties of the species formed in the solution including size of hydration, draw solution viscosity, solubility and charge. In general reverse solute flux of $MgSO_4$ contains divalent ions which lower reverse solute flux because of lower diffusivity for water treatment using forward osmosis application [65, 66].

3.7.5. Fouling studies of all membranes

The reverse solute fluxes while fouling the membranes using 50 ppm humic acid was studied. The results are shown in Figure12, fouling is the accumulation of organic matter on the surface of the membrane, thereby reducing water permeation leading to reduced flux. The effect of adding humic acid on the feed solution resulted in a decline in reverse solute water flux. In Figure 12, the membrane with 0.1 wt.% QCNTs for both NaCl and $MgSO_4$ as a draw solute was 5.72 $L.m^{-2}h^{-1}$ and 5.03 $L.m^{-2}h^{-1}$ with a flux of 30% and 37.6% respectively this was declined compared to Figure 11. This initial decline can be attributed to the adsorption of humic acid on the surface of the membrane upon the initial introduction of the solution. The membrane with 0.1 wt.% QCNTs was still the best performing membrane. This indicated that the membrane was not easily fouled; the hydrophilicity of the QCNTs reduced the fouling ability of the membrane.

Upon increasing QCNTs loading, the reverse solute fluxes decreased after fouling. The decrease is related to the membrane hydrophilicity, the membrane is easily fouled due to its low hydrophilicity as per Figure 9. The humic acid easily fouled the membrane due to the agglomeration of QCNTs. Agglomeration renders the membranes ineffective. Motsa et al. [67] indicated that a high fouling propensity causes a flux decline due to the low osmotic driving force created by the feed solution increased internal concentration polarization which is why the membranes with 0.3 and 0.5 wt.% reported low revers solute fluxes.

4. Conclusions

Quaternized polyethersulfone membranes blended with quaternized carbon nanotubes were successfully prepared via phase inversion method. These membranes were tested using forward osmosis application for brackish water desalination. The addition of QCNTs increased the hydrophilicity of the membranes. The blend membrane with magnesium sulfate as a draw solute was found to be dependent on the amount of QCNTs added. The flux of the

pristine membrane was 7.24 $L.m^{-2}h^{-1}$ and 8.06 $L.m^{-2}h^{-1}$ for quaternized membrane. However, as flux increased, rejection decreased as compared to pure membrane without quaternized CNTs. This is due to the opening of pores and macro voids observed from the morphological analysis of the membrane.

The effect of reverse solute flux on the performance of the membrane was also evaluated. Increase in reverse solute flux decreases the performance of the membrane during operation due to the solute that has built up on the feed draw solution. The QCNTs also reduce the fouling ability of the membrane. This allows the membrane to be used for a longer time while rejecting the salt. This work has successfully demonstrated that QPES/QCNTs can be used for FO application. Even though the flux of the FO membrane is still a significant factor of the process which needs a lot of research studies. There was a small increase of flux 8.06 $Lm^{-2}h^{-1}$ in the FO which will shorten the life span of the membrane due to internal concentration polarization. It should also be noted that the osmotic pressure for this study at 1M and 2M was 24 bar and 48.9 bar. The concentration used in this study was supposed to result in a double flux than the obtained one (8.06 $Lm^{-2}h^{-1}$), this indicates that membrane properties improvement is still required, nevertheless the membrane showed improved properties than the pristine membrane.

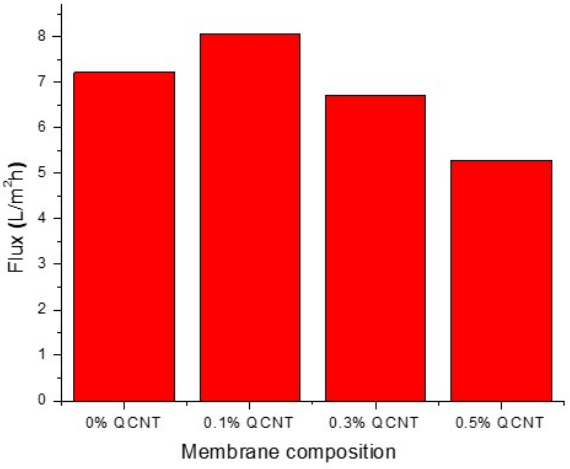

Fig. 10. Pure water flux of PES and composite membranes.

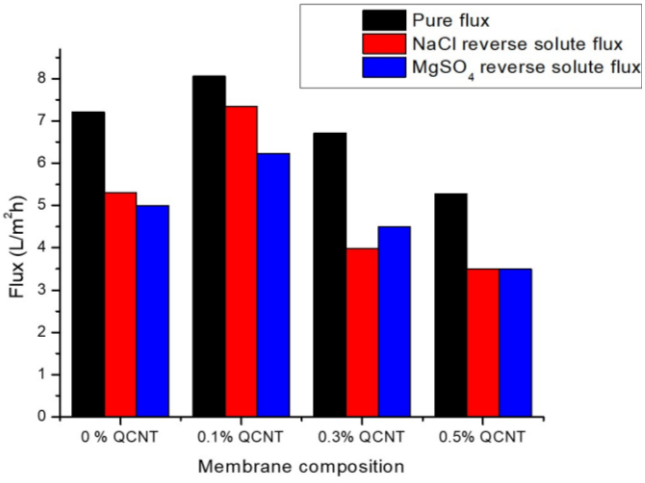

Fig. 11. Reverse solute flux of QPES /QCNT blend membranes.

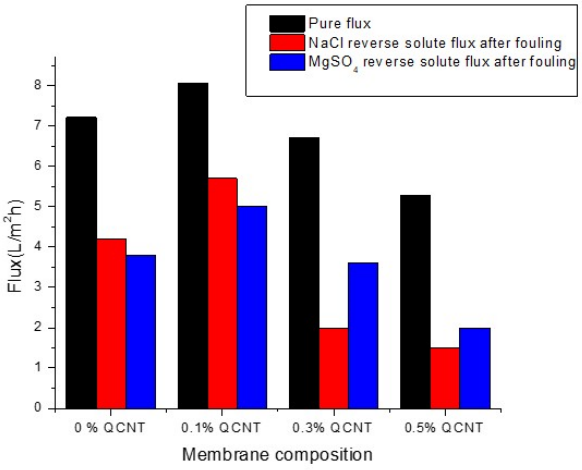

Fig. 12. Reverse solute flux after fouling for all membranes.

Acknowledgement

The authors are thankful to South African Department of science and technology Nanotechnology Innovation Centre (DST/NIC-Mintek) and the University of Johannesburg for financial support. Authors are also thankful to the Centre for Nanomaterials Science Research (CNSR) at the University of Johannesburg for additional and National Research foundation for additional funding support.

References

[1] V.G. Gude, Desalination and water reuse to address global water scarcity, Reviews in Environmental Science and Bio/Technology, 16 (2017) 591-609. DOI: 10.1007/s11157-017-9449-7

[2] P. Levallois, C.M. Villanueva, Drinking Water Quality and Human Health: An Editorial, in,Multidisciplinary Digital Publishing Institute, 2019. DOI: https://doi.org/10.3390/ijerph16040631

[3] J. Edokpayi, E. Rogawski, D. Kahler, C. Hill, C. Reynolds, E. Nyathi, J. Smith, J. Odiyo, A. Samie, P. Bessong, Challenges to sustainable safe drinking water: a case study of water quality and use across seasons in rural communities in Limpopo province, South Africa, Water, 10 (2018) 159. DOI: https://doi.org/10.3390/w10020159

[4] S. Roy, S. Ragunath, Emerging membrane technologies for water and energy sustainability: Future prospects, constraints and challenges, Energies, 11 (2018) 2997. DOI: https://doi.org/10.3390/en11112997

[5] Y. Yu, S. Seo, I.-C. Kim, S. Lee, Nanoporous polyethersulfone (PES) membrane with enhanced flux applied in forward osmosis process, Journal of membrane science, 375 (2011) 63-68. DOI: https://doi.org/10.1016/j.memsci.2011.02.019

[6] S. Roy, S. Ragunath, Emerging Membrane Technologies for Water and Energy Sustainability: Future Prospects, Constrains and Challenges, Energies, 11 (2018) 1-32. DOI: https://doi.org/10.3390/en11112997

[7] Z.-X. Low, Q. Liu, E. Shamsaei, X. Zhang, H. Wang, Preparation and characterization of thin-film composite membrane with nanowire-modified support for forward osmosis process, Membranes, 5 (2015) 136-149. DOI: https://doi.org/10.3390/membranes5010136

[8] I. Alsvik, M.-B. Hägg, Pressure retarded osmosis and forward osmosis membranes: materials and methods, Polymers, 5 (2013) 303-327. DOI: https://doi.org/10.3390/polym5010303

[9] M. Shaban, A.M. Ashraf, H. AbdAllah, H.A. El-Salam, Titanium dioxide nanoribbons/multi-walled carbon nanotube nanocomposite blended polyethersulfone membrane for brackish water desalination, Desalination, 444 (2018) 129-141. DOI: https://doi.org/10.1016/j.desal.2018.07.006

[10] N. Maximous, G. Nakhla, W. Wan, K. Wong, Preparation, characterization and performance of Al2O3/PES membrane for wastewater filtration, Journal of Membrane Science, 341 (2009) 67-75. DOI: https://doi.org/10.1016/j.memsci.2009.05.040

[11] E. Celik, H. Park, H. Choi, H. Choi, Carbon nanotube blended polyethersulfone membranes for fouling control in water treatment, Water research, 45 (2011) 274-282. DOI: https://doi.org/10.1016/j.watres.2010.07.060

[12] K. Nikita, P. Karkare, D. Ray, V. Aswal, P.S. Singh, C. Murthy, Understanding the morphology of MWCNT/PES mixed-matrix membranes using SANS: interpretation and rejection performance, Applied Water Science, 9 (2019) 154. DOI: https://doi.org/10.1007/s13201-019-1035-4

[13] F. Khoerunnisa, D.R. Primastari, R. Agiawati, Effect of MWCNT Filler on

Properties and Flux of Chitosan/PEG based Nanocomposites Membranes, in: MATEC Web of Conferences, EDP Sciences (2018) 04001. DOI: https://doi.org/10.1051/matecconf/201815604001

[14] J. Lin, W. Ye, K. Zhong, J. Shen, N. Jullok, A. Sotto, B. Van der Bruggen, Enhancement of polyethersulfone (PES) membrane doped by monodisperse Stöber silica for water treatment, Chemical Engineering and Processing-Process Intensification, 107 (2016) 194-205. DOI: https://doi.org/10.1016/j.cep.2015.03.011

[15] R. Sengur-Tasdemir, V.R. Mokkapati, D.Y. Koseoglu-Imer, I. Koyuncu, Effect of polymer type on characterization and filtration performances of multi-walled carbon nanotubes (MWCNT)-COOH-based polymeric mixed matrix membranes, Environmental technology, 39 (2018) 1226-1237. DOI: https://doi.org/10.1080/09593330.2017.1325409

[16] A. Aende, J. Gardy, A. Hassanpour, Seawater Desalination: A Review of Forward Osmosis Technique, Its Challenges, and Future Prospects, Processes, 8 (2020) 901.

[17] L. Wu, T. Xu, D. Wu, X. Zheng, Preparation and characterization of CPPO/BPPO blend membranes for potential application in alkaline direct methanol fuel cell, Journal of Membrane Science, 310 (2008) 577-585. DOI: https://doi.org/10.3390/pr8080901

[18] N. Lodhi, N.K. Mehra, N.K. Jain, Development and characterization of dexamethasone mesylate anchored on multi walled carbon nanotubes, Journal of drug targeting, 21 (2013) 67-76. DOI: https://doi.org/10.3109/1061186X.2012.729213

[19] M.A. Hossain, H. Jang, S.C. Sutradhar, J. Ha, J. Yoo, C. Lee, S. Lee, W. Kim, Novel hydroxide conducting sulfonium-based anion exchange membrane for alkaline fuel cell applications, International Journal of Hydrogen Energy, 41 (2016) 10458-10465. DOI: https://doi.org/10.1016/j.ijhydene.2016.01.051

[20] R. Saranya, G. Arthanareeswaran, D.D. Dionysiou, Treatment of paper mill effluent using polyethersulfone/functionalised multiwalled carbon nanotubes based nanocomposite membranes, Chemical Engineering Journal, 236 (2014) 369-377. DOI: https://doi.org/10.1016/j.cej.2013.09.096

[21] N. Dementev, R. Ronca, E. Borguet, Oxygen-containing functionalities on the surface of multi-walled carbon nanotubes quantitatively determined by fluorescent labeling, Applied Surface Science, 258 (2012) 10185-10190. DOI: https://doi.org/10.1016/j.apsusc.2012.06.103

[22] C. Kahattha, P. Woointranont, T. Chodjarusawad, W. Pecharapa, Study of acid-treated multiwall carbon nanotubes by electron microscopy and raman spectroscopy, Journal of the Microscopy Society of Thailand, 24 (2010) 133.

[23] S.A. Shamsuddin, M.N. Derman, U. Hashim, M. Kashif, T. Adam, N.H.A. Halim, M.F.M. Tahir, Nitric acid treated multi-walled carbon nanotubes optimized by Taguchi method, in: AIP Conference Proceedings, AIP Publishing LLC (2016) 090002. DOI: https://doi.org/10.1063/1.4958783

[24] M.A. Motchelaho, H. Xiong, M. Moyo, L.L. Jewell, N.J. Coville, Effect of acid treatment on the surface of multiwalled carbon nanotubes prepared from Fe–Co supported on $CaCO_3$: correlation with Fischer–Tropsch catalyst activity, Journal of Molecular Catalysis A: Chemical, 335 (2011) 189-198. DOI: https://doi.org/10.1016/j.molcata.2010.11.033

[25] J.H. Lehman, M. Terrones, E. Mansfield, K.E. Hurst, V. Meunier, Evaluating the characteristics of multiwall carbon nanotubes, Carbon, 49 (2011) 2581-2602. DOI: https://doi.org/10.1016/j.carbon.2011.03.028

[26] M.A. Akl, A.M. Abou-Elanwar, Adsorption studies of cd (II) from water by acid modified multiwalled carbon nanotubes, Journal of Nanomedicine & Nanotechnology, 6 (2015) 1. DOI: 10.4172/2157-7439.1000327

[27] S. Botti, A. Rufoloni, T. Rindzevicius, M.S. Schmidt, Surface-Enhanced Raman Spectroscopy Characterization of Pristine and Functionalized Carbon Nanotubes and Graphene, in: Raman Spectroscopy, InTechOpen, 2018, pp. 203-219. DOI: https://doi.org/10.1016/j.jallcom.2019.04.177

[28] H. Zhao, S. Qiu, L. Wu, L. Zhang, H. Chen, C. Gao, Improving the performance of polyamide reverse osmosis membrane by incorporation of modified multi-walled carbon nanotubes, Journal of Membrane Science, 450 (2014) 249-256. DOI: https://doi.org/10.1016/j.memsci.2013.09.014

[29] T.M. Le Hoa, Characterization of multi-walled carbon nanotubes functionalized by a mixture of HNO3/H2SO4, Diamond and Related Materials, 89 (2018) 43-51. DOI: 10.1016/j.diamond.2018.08.008

[30] B. Maciejewska, M. Jasiurkowska-Delaporte, A. Vasylenko, K. Kozioł, S. Jurga, Experimental and theoretical studies on the mechanism for chemical oxidation of multiwalled carbon nanotubes, RSC Advances, 4 (2014) 28826-28831. DOI: https://doi.org/10.1039/C4RA03881A

[31] A. Jimeno, S. Goyanes, A. Eceiza, G. Kortaberria, I. Mondragon, M. Corcuera, Effects of amine molecular structure on carbon nanotubes functionalization, Journal of nanoscience and nanotechnology, 9 (2009) 6222-622. DOI: DOI: https://doi.org/10.1166/jnn.2009.1562

[32] K. Osler, D. Dheda, J. Ngoy, N. Wagner, M.O. Daramola, Synthesis and evaluation of carbon nanotubes composite adsorbent for CO 2 capture: a comparative study of CO 2 adsorption capacity of single-walled and multi-walled carbon nanotubes, International Journal of Coal Science & Technology, 4 (2017) 41-49. DOI: 10.1007/s40789-017-0157-2

[33] A. Rufoloni, L. Mezi, S. Botti, Surface-enhanced Raman spectroscopy characterisation of functionalised multi-walled carbon nanotubes, (2015). DOI: https://doi.org/10.1039/C4CP05075D

[34] W.M. Silva, H. Ribeiro, L.M. Seara, H.D. Calado, A.S. Ferlauto, R.M. Paniago, C.F. Leite, G.G. Silva, Surface properties of oxidized and aminated multi-walled carbon nanotubes, Journal of the Brazilian Chemical Society, 23 (2012) 1078-1086. DOI: http://dx.doi.org/10.1590/S0103-50532012000600012

[35] M. Masheane, A. Verliefde, S. Mhlanga, PES/Quaternized-PES Blend Anion Exchange Membranes: Investigation of Polymer Compatibility and Properties of the Blend, Journal of Membrane Science & Research, (2018). DOI: DOI: 10.22079/JMSR.2018.74701.1163

[36] R. Kalaivizhi, Preparation of polymer blend membranes based on cellulose acetate and quaternized polyethersulfone for ultrafiltration, International Journal of Green Pharmacy (IJGP), 12 (2018).

[37] P.F. Msomi, P. Nonjola, P.G. Ndungu, J. Ramonjta, Quaternized poly (2.6 dimethyl-1.4 phenylene oxide)/polysulfone blend composite membrane doped with Z n O-nanoparticles for alkaline fuel cells, Journal of Applied Polymer Science, 135 (2018) 45959. DOI: https://doi.org/10.1002/app.45959

[38] G. Das, C.Y. Kim, D.H. Kang, B.H. Kim, H.H. Yoon, Quaternized Polysulfone Cross-Linked N, N-Dimethyl Chitosan-Based Anion-Conducting Membranes, Polymers, 11 (2019) 512. DOI: https://doi.org/10.3390/polym11030512

[39] S.S. Koilpillai, S. Dharmalingam, A novel quaternized poly (ether sulfone) membrane for alkaline fuel cell application, International Journal of Energy Research, 39 (2015) 317-325. https://doi.org/10.1002/er.3240

[40] T. Huang, M. Zhang, L. Cheng, L. Zhang, M. Huang, Q. Xu, H. Chen, A novel polysulfone-based affinity membrane with high hemocompatibility: preparation and endotoxin elimination performance, RSC Advances, 3 (2013) 25982-25988. DOI: https://doi.org/10.1039/C3RA43594F

[41] V. Subramanian, O. Gupte, Functionalization of poly (ether sulfone) (PES) and polysulfone (PSF) membrane, The Bombay Technologist, 64 (2014) 22-26.

[42] D. Xing, S. Zhang, C. Yin, C. Yan, X. Jian, Preparation and characterization of chloromethylated/quanternized poly (phthalazinone ether sulfone) anion exchange membrane, Materials Science and Engineering: B, 157 (2009) 1-5. DOI: https://doi.org/10.1016/j.mseb.2008.11.019

[43] S. Zhu, G. Xiao, D. Yan, Synthesis of aromatic polyethersulfone-based graft copolyacrylates via ATRP catalyzed by $FeCl_2$/isophthalic acid, Journal of Polymer Science Part A: Polymer Chemistry, 39 (2001) 2943-2950. DOI: https://doi.org/10.1002/pola.1275

[44] W. Chen, X. Yan, X. Wu, S. Huang, Y. Luo, X. Gong, G. He, Tri-quaternized poly (ether sulfone) anion exchange membranes with improved hydroxide conductivity, Journal of Membrane Science, 514 (2016) 613-621. DOI: https://doi.org/10.1016/j.memsci.2016.05.004

[45] M.N.Z. Abidin, P.S. Goh, A.F. Ismail, M.H.D. Othman, H. Hasbullah, N. Said, S.H.S.A. Kadir, F. Kamal, M.S. Abdullah, B.C. Ng, Antifouling polyethersulfone hemodialysis membranes incorporated with poly (citric acid) polymerized multi-walled carbon nanotubes, Materials Science and Engineering: C, 68 (2016) 540-550. DOI: https://doi.org/10.1016/j.msec.2016.06.039

[46] A. Najjar, S. Sabri, R. Al-Gaashani, M.A. Atieh, V. Kochkodan, Antibiofouling performance by polyethersulfone membranes cast with oxidized multiwalled carbon nanotubes and Arabic gum, Membranes, 9 (2019) 32. DOI: https://doi.org/10.3390/membranes9020032

[47] M.S. Rameetse, O. Aberefa, M.O. Daramola, Effect of Loading and Functionalization of Carbon Nanotube on the Performance of Blended Polysulfone/Polyethersulfone Membrane during Treatment of Wastewater Containing Phenol and Benzene, Membranes, 10 (2020) 54. DOI: https://doi.org/10.3390/membranes10030054

[48] D.L. Arockiasamy, J. Alam, M. Alhoshan, Carbon nanotubes-blended poly (phenylene sulfone) membranes for ultrafiltration applications, Applied Water Science, 3 (2013) 93-103. DOI: 10.1007/s13201-012-0063-0

[49] S. Loganathan, R.B. Valapa, R.K. Mishra, G. Pugazhenthi, S. Thomas, Thermogravimetric analysis for characterization of nanomaterials, in: Thermal and Rheological Measurement Techniques for Nanomaterials Characterization, Elsevier, 2017, pp. 67-108. DOI: https://doi.org/10.1016/B978-0-323-46139-9.00004-9

[50] C.E. Corcione, M. Frigione, Characterization of nanocomposites by thermal analysis, Materials, 5 (2012) 2960-2980. DOI: https://doi.org/10.3390/ma5122960

[51] P. Shah, C. Murthy, Studies on the porosity control of MWCNT/polysulfone composite membrane and its effect on metal removal, Journal of membrane science, 437 (2013) 90-98. DOI: https://doi.org/10.1016/j.memsci.2013.02.042

[52] A. Khalid, A. Abdel-Karim, M.A. Atieh, S. Javed, G. McKay, PEG-CNTs nanocomposite PSU membranes for wastewater treatment by membrane bioreactor, Separation and Purification Technology, 190 (2018) 165-176. DOI: https://doi.org/10.1016/j.seppur.2017.08.055

[53] R. Kumar, M. Ahmed, B. Garudachari, J.P. Thomas, Evaluation of the Forward Osmosis Performance of Cellulose Acetate Nanocomposite Membranes, Arabian Journal for Science and Engineering, 43 (2018) 5871-5879. DOI: https://doi.org/10.1007/s13369-017-3048-3

[54] Y. Zhang, L. Shi, G. Li, S. Liang, Impact of Functional Groups in MWCNT on Surface Hydrophilicity, Mechanical and Thermal Properties of Polystyrene/CNT Composites, in: IOP Conference Series: Materials Science and Engineering, IOP Publishing, 2017, pp. 012052. DOI: 10.1088/1757-899X/250/1/012052

[55] M. Giagnorio, F. Ricceri, A. Tiraferri, Desalination of brackish groundwater and reuse of wastewater by forward osmosis coupled with nanofiltration for draw solution recovery, Water research, 153 (2019) 134-143. DOI: https://doi.org/10.1016/j.watres.2019.01.014

[56] S.-J. Im, J. Choi, S. Jeong, A. Jang, New concept of pump-less forward osmosis (FO) and low-pressure membrane (LPM) process, Scientific reports, 7 (2017) 1-6. DOI:10.1038/s41598-017-15274-z

[57] Q. Liu, J. Li, Z. Zhou, J. Xie, J.Y. Lee, Hydrophilic mineral coating of membrane substrate for reducing internal concentration polarization (ICP) in forward osmosis, Scientific reports, 6 (2016) 19593. DOI: 10.1038/srep19593

[58] A. Ambrosi, G. Lopes Corrêa, N. Souza de Vargas, L. Martim Gabe, N.S.M. Cardozo, I.C. Tessaro, Impact of osmotic agent on the transport of components using forward osmosis to separate ethanol from aqueous solutions, AIChE Journal, 63 (2017) 4499-4507. DOI: https://doi.org/10.1002/aic.15779

[59] J.S. Yong, W.A. Phillip, M. Elimelech, Coupled reverse draw solute permeation and water flux in forward osmosis with neutral draw solutes, Journal of Membrane Science, 392 (2012) 9-17. DOI: https://doi.org/10.1016/j.memsci.2011.11.020

[60] S.K. Yen, M. Su, K.Y. Wang, T.-S. Chung, Study of draw solutes using 2-methylimidazole-based compounds in forward osmosis, Journal of Membrane Science, 364 (2010) 242-252. DOI: https://doi.org/10.1016/j.memsci.2010.08.021

[61] Q. She, X. Jin, Q. Li, C.Y. Tang, Relating reverse and forward solute diffusion to membrane fouling in osmotically driven membrane processes, Water research, 46 (2012) 2478-2486. DOI: https://doi.org/10.1016/j.watres.2012.02.024

[62] J. Alam, L.A. Dass, M. Ghasemi, M. Alhoshan, Synthesis and optimization of PES-Fe3O4 mixed matrix nanocomposite membrane: Application studies in water purification, Polymer composites, 34 (2013) 1870-1877. DOI: https://doi.org/10.1002/pc.22593

[63] J.-G. Gai, X.-L. Gong, Zero internal concentration polarization FO membrane: functionalized graphene, Journal of Materials Chemistry A, 2 (2014) 425-429. DOI: https://doi.org/10.1039/C3TA13562D

[64] N. Akther, A. Sodiq, A. Giwa, S. Daer, H. Arafat, S. Hasan, Recent advancements in forward osmosis desalination: a review, Chemical Engineering Journal, 281 (2015) 502-522. DOI: https://doi.org/10.1016/j.cej.2015.05.080

[65] R.W. Holloway, R. Maltos, J. Vanneste, T.Y. Cath, Mixed draw solutions for improved forward osmosis performance, Journal of membrane science, 491 (2015) 121-131. DOI: https://doi.org/10.1016/j.memsci.2015.05.016

[66] S. Phuntsho, H.K. Shon, S. Hong, S. Lee, S. Vigneswaran, J. Kandasamy, Fertiliser drawn forward osmosis desalination: the concept, performance and limitations for fertigation, Reviews in Environmental Science and Bio/Technology, 11 (2012) 147-168. DOI: 10.1007/s11157-011-9259-2

[67] M.M. Motsa, B.B. Mamba, A. D'Haese, E.M. Hoek, A.R. Verliefde, Organic fouling in forward osmosis membranes: The role of feed solution chemistry and membrane structural properties, Journal of Membrane Science, 460 (2014) 99-109. DOI: 10.1007/s11157-017-9449-7